Ion Transport in the Gramicidin Channel: Free Energy of the Solvated Right-Handed Dimer in a Model Membrane†

Benoît Roux and Martin Karplus*

Contribution from the Department of Chemistry, Harvard University, Cambridge, Massachusetts 02138

Received July 13, 1992

Abstract: The free energy profile of a Na^+ ion along the axis of the gramicidin A dimer channel is calculated by molecular dynamics simulations. A cylindrical system is used that is based on a detailed atomic model of the gramicidin dimer, which is solvated at both ends of the channel and surrounded by a simplified model membrane. The entire system consists of 967 atoms and is treated with cylindrical periodic boundary conditions. The gramicidin channel was modeled from the right-handed head-to-head β-helix dimer determined experimentally by two-dimensional NMR. Simulations were made to estimate the free energy profile in three regions: the transition from bulk-like solvation to single file, the single-file region at the entrance of the channel, and the intermonomer junction of the dimer channel. In each region, approximate corrections are introduced to account for hysteresis effects in the simulations. Binding sites are found at the extremities of the channel in agreement with experiment. The principal energy barrier is at the entrance of the channel in the single-file region. No large activation energy barrier is introduced by the dehydration process, because the transformation from bulk to single-file solvation is progressive and takes place over a distance of 5–6 Å. The free energy simulation results obtained in this paper are joined with those calculated from a periodic model of the interior of the pore to construct an approximate free energy profile of the entire channel system.

Introduction

The gramicidin channel is the most studied and best understood ion-permeable channel.[1,2] Because it exhibits functional behavior similar to the more complex biological channels, while being relatively small and structurally well-characterized, the gramicidin channel has been the model of choice for studies of the mechanisms of ionic permeation across lipid membranes. Increasing experimental information about the conductance and selectivity of chemically modified gramicidin channels is being obtained.[3-6] This is a promising area in rapid development that could lead to an understanding of the general principles of ion channel conductance and serve as a basis for the rational modification and design of such channels.

The gramicidin channel is well-suited for theoretical study because of its structural and functional simplicity. Moreover, many important questions about the permeation process through the gramicidin channel remain unanswered. In particular, the lack of detailed knowledge about the location of the binding sites and the rate-limiting activation barriers prevents definitive conclusions from being drawn from the experimental observations. Work on the gramicidin channel has now reached the point where the design and interpretation of experiments can be aided by theoretical calculations to develop a realistic and detailed microscopic picture of ion permeation.

The goal of the present study is to provide additional information for calculating the free energy profile of Na^+ along the channel axis of a detailed atomic model of gramicidin. Previous studies[7,8] of a gramicidin-like periodic β-helix suggested that the free energy profile of the Na^+ ion in the interior of a monomer is made of a sequence of small wells and energy barriers separated by 1.55 Å, the distance between two successive (L,D) helical units, independent of the handedness of the helix. In this paper we extend the calculation of the free energy profile into three regions of the channel that may be expected to differ markedly from a periodic β-helix: (I) the transition from bulk solvation to single file; (II) the single-file region at the entrance of the channel; and (III) the intermonomer junction at the center of the dimer channel. The results of the present calculations are joined with the periodic β-helix analysis for the channel interior[7] to obtain an estimate of the full energy profile for the solvated dimer channel.

The gramicidin channel was constructed as a right-handed head-to-head dimer. The right-handedness of the gramicidin dimer has been demonstrated experimentally by two-dimensional proton–proton NOE spectroscopy of the dimer incorporated into sodium dodecyl sulfate micelles (SDS)[9] and by solid-state ^{15}N NMR of the dimer incorporated into an oriented dimyristoylphosphatidylcholine (DMPC) bilayer preparation.[10] However, there also exists evidence for a left-handed head-to-head dimer in lysolecithin phospholipid structures.[11] In view of the sensitivity of gramicidin to the environment,[12] it may well be that both structures exist and that one or the other is more stable depending on the composition of the lipid membrane. As yet, no conductance studies have been made for the lipid system in which the right-handed helix has been shown to exist. Although we have chosen the right-handed dimer for study in this paper, molecular dynamics simulations of solvated right- and left-handed dimers indicate that the properties of the two structures are very similar.[13]

The details of the microscopic model and of the empirical energy function are introduced in the next section, which also describes

† Supported in part by a grant from the National Science Foundation.

(1) Andersen, O. S. *Annu. Rev. Physiol.* **1984**, *46*, 531.
(2) Hille, B. Ionic Channels of Excitable Membranes; Sinauer: Sunderland, MA, 1984.
(3) Mazet, J. L.; Andersen, O. S.; Koeppe, R. E., II. *Biophys. J.* **1984**, *45*, 263.
(4) Andersen, O. S.; Koeppe, R. E., II; Durkin, J. T.; Mazet, J. L. In Ion transport through membranes; Academic Press: New York, 1987; p 295.
(5) Koeppe, R. E., II; Andersen, O. S.; Maddock, A. K. In Transport through membranes: Carriers, channels, and pumps; Pullman, A., et al., Eds.; Kluwer Academic Publisher: Dordrecht, The Netherlands, 1988; p 133.
(6) Becker, M. D.; Greathouse, D. V.; Koeppe, R. E.; Andersen, O. S. *Biochemistry* **1991**, *30*, 8830.
(7) Roux, B.; Karplus, M. *Biophys. J.* **1991**, *59*, 961.
(8) Roux, B.; Karplus, M. *J. Phys. Chem.* **1991**, *95*, 4856.
(9) Arseniev, A. S.; Bystrov, V. F.; Ivanov, T. V.; Ovchinnikov, Y. A. *FEBS Lett.* **1985**, *186*, 168.
(10) Nicholson, L. K.; Cross, T. A. *Biochemistry* **1989**, *28*, 9379.
(11) Urry, D. W.; Trapane, T. L.; Prasad, K. U. *Science* **1983**, *221*, 1064.
(12) Arseniev, A. S.; Barsukov, I. L.; Bystrov, V. F.; Lomize, A. L.; Ovchinnikov, Yu. A. *FEBS Lett.* **1984**, *165*, 51.
(13) Roux, B.; Karplus, M. The dynamics of water in the gramicidin channel. In preparation.

0002-7863/93/1515-3250$04.00/0

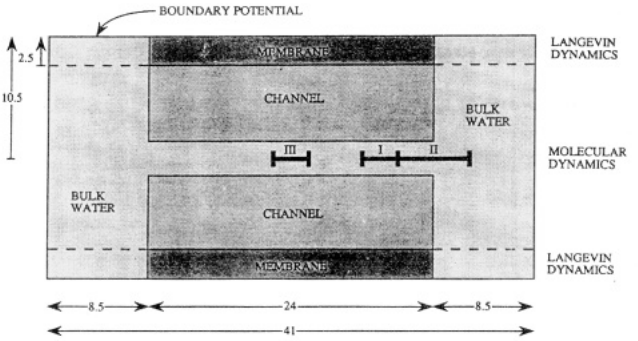

Figure 1. Schematic representation of the simulation system that shows the dimer channel, the bulk water, and the model membrane. All dimensions are given in angstroms. The boundary potential applied in the radial direction and the Langevin regions are indicated. Water molecules within 2.5 Å of the surface of the cylinder and all the membrane spheres obey Langevin dynamics, the remaining atoms obey pure molecular dynamics. The x-axis is parallel to the channel axis, and $x = 0$ is located at the center of the dimer. The three regions of the free energy profile are shown: (I) the beginning of the single-file solvation at the entrance of the channel ($6.02 \leq x \leq 9.17$); (II) the transition from single-file bulk solvation ($9.17 \leq x \leq 14.57$); and (III) the intermonomer junction at the center of the dimer channel ($-1.05 \leq x \leq 1.05$).

the free energy perturbation technique and the simulation procedure. Results for the free energy profile in the entrance and dimer junction are described subsequently. The structural aspects of the translocation inside the gramicidin channel and the dehydration process of the Na^+ ion at the channel entrance and at the monomer junction are analyzed. Because of hysteresis effects in the simulation results, corrections are introduced to obtain an estimate of the full-converged values. From earlier results on the interior of the channel, based on the periodic helix model,[7] and the present simulations, an approximate free energy profile of Na^+ along the axis of the gramicidin channel is constructed. Although the free energy profile is not a quantitative theoretical prediction, its general aspect is likely to be correct and should, therefore, be useful for interpreting experimental data. Appendix A shows that the error introduced by use of a finite system is small. Appendix B gives the detailed simulation results, and Appendix C presents the point by point results for the calculated free energy profile for the Na^+ ion in the channel.

Methodology

Microscopic Model. The main features of the simulation system and its dimensions are illustrated schematically in Figure 1. The gramicidin channel was constructed as a right-handed head-to-head dimer from the coordinates determined experimentally by proton–proton NOE distances;[9,14] both the backbone and side-chain atoms were included using a polar hydrogen model. The primary solvation of the channel was provided by 24 water molecules, of which 12 were located along the pore axis separated by a distance of 2.8 Å and 6 were at each extremity of the channel. The positions of the 6 water molecules at each extremity were optimized with energy minimization in the presence of a restraining harmonic potential to force them to fill the mouths of the channel. The bulk-like water regions were constructed by overlaying water molecules taken from the coordinates of a box of TIP3P water equilibrated at 300 K[15] and deleting the water molecules overlapping with the channel or the first 24 waters. To produce a hydrocarbon-like environment and to prevent waters from reaching the lateral side of the dimer, a model "membrane" is included. It is composed of Lennard-Jones (LJ) spheres (no charge or polarizability) corresponding to the size of a CH_3 group ($r_{min} = 2.165$ Å, $\epsilon = -0.1811$ kcal/mol). A similar overlay method was used to construct the model membrane from a box of the spheres at approximately the same density as bulk water. The initial system consists of 314 peptide atoms for the gramicidin dimer, 190 TIP3P water molecules,[15] and 85 LJ spheres. One water molecule was substituted by a Na^+ ion to construct the systems used for the free energy calculations. There are 967 particles in the ion–channel system. Periodic boundary conditions were applied along the channel axis to mimic the effect of infinite bulk water. A confining potential, analogous to that employed in stochastic spherical boundary simulations,[16] was determined for the cylindrical geometry of the system and was applied in the radial direction on the water oxygens to maintain proper density in the bulk-like regions. The center of mass of the dimer was placed at the origin with the channel oriented along the x-axis. The diameter of the cylindrical system is 21 Å, and the length of the elementary unit is 41 Å, going from $x = -20.5$ Å to $x = +20.5$ Å. The transition from the pore to the bulk-like region is approximately located at $x = \pm 12$ Å. No water molecules are located on the lateral sides of the channel between +12 and −12 Å. A weak harmonic constraint of 0.6 kcal/(mol Å) was applied to the Lennard-Jones membrane spheres to prevent them from diffusing into the bulk water region. Water molecules within 2.5 Å of the surface of the cylinder and all the LJ spheres were submitted to dissipative and stochastic Langevin forces corresponding to a velocity relaxation rate of 62 ps^{-1}. Due to the significant contribution of electrostatic energy terms to the interactions of the ion, a relatively large nonbonded group-by-group-based cutoff of 12 Å was used with a smooth switching region of 4 Å. The water–water (TIP3P),[15] peptide–peptide (CHARMM),[17] and water–peptide[18] potential functions used have been described elsewhere. Special care was given to the parametrization of the interaction of the ion with the channel. From ab initio calculations with Na^+ and acetamide,[7,19] it was found that a good description of the sodium ion–channel atom interactions includes a van der Waals core term, an electrostatic interaction between the ion and the partial charge of the peptide atoms, and a charge-induced dipole interaction varying as $1/r^4$ as a function of ion–peptide atoms distance; all heavy atoms of the backbone interact with the ion by the charge–charge and charge-induced dipole potential. The ion–carbonyl oxygen core interaction is represented by a modified $1/r^8$ core repulsion, softer than the more standard Lennard-Jones 6–12 potential. Only the first-order polarization induced by the ion was included in the calculation (i.e. the induced dipoles were not calculated self-consistently with the total electric field) to maintain consistency with the CHARMM[17] and TIP3P[15] force fields. The integration time step for the dynamics was 0.001 ps.

Reaction Coordinate and Perturbation Technique. From Boltzmann statistics, the free energy of the system, W, as a function of the reaction coordinate $\zeta(R)$ is given by the multidimensional configuration integrals over all degrees of freedom R in the system;[20] i.e.,

$$e^{-[W(\zeta)-W(\zeta_O)]/k_BT} = \frac{\int dR\, \delta(\zeta'[R] - \zeta) e^{-U(R)/k_BT}}{\int dR\, \delta(\zeta'[R] - \zeta_O) e^{-U(R)/k_BT}} \quad (1)$$

where $U(R)$ is the interaction potential energy of the system and the δ function ensures that the reaction coordinate function $\zeta'[R]$ is constrained at the position ζ. From eq 1, the free energy profile is determined relative to the position ζ_O and depends on the value of $W(\zeta_O)$, a constant related to the absolute free energy of the ion in the channel. Since our goal is to compute the relative free energy of the ion along the axis of the channel, the value of $W(\zeta_O)$ remains arbitrary in the present calculation. The choice of a reaction coordinate for describing the dynamical properties in a complex multidimensional dense system is not unique.[21] However, once the reaction coordinate is chosen, the projection of the potential energy $U(R)$ onto a one-dimensional potential-of-mean force, $W(\zeta)$, can be calculated for an arbitrary choice of function $\zeta'[R]$ from eq 1.[20] It is important to identify the slow and fast motions that are responsible for the separation of time scales in the system such that the dynamic "orthogonal" to ζ relaxes much more rapidly than that "parallel" to ζ.[22] This ensures that the transmission coefficient for barrier crossing is as close to unity as possible and that the rates are primarily determined by

(14) Arseniev, A. S.; Barsukov, I. L.; Bystrov, V. F. In Chemistry of peptides and proteins 3; Voelter, W., Bayer, E., Ovchinnikov, Y. A., Ivanov, V. T., Eds.; W. Voelter Co., Berlin, Germany, 1986; p 127.

(15) Jorgensen, W. L.; Chandrasekhar, J.; Madura, J. D.; Impey, R. W.; Klein, M. L. *J. Chem. Phys.* **1983**, *79*, 926.

(16) Brooks, C. L., III; Karplus, M. *J. Chem. Phys.* **1983**, *79*, 6312.

(17) Brooks, B. R.; Bruccoleri, R. E.; Olafson, B. D.; States, D. J.; Swaminathan, S.; Karplus, M. *J. Comput. Chem.* **1983**, 4187.

(18) Reiher, W. E., III; Karplus, M. Theoretical studies of hydrogen bonding. In preparation.

(19) Roux, B.; Karplus, M. Empirical energy function for cations-peptides interactions. In preparation.

(20) McQuarrie, D. A. Statistical Mechanics; Harper and Row: New York, 1976.

(21) Hynes, J. T. In Theory of chemical reaction dynamics; Baer, M., Ed.; CRC Press: Boca Raton, FL, 1985; p 171.

(22) Berne, B. J.; Pecora, R. Dynamic Light Scattering; Wiley-Interscience: New York, 1976.

the activation energy as in transition-state theory.[23] It is also desirable to choose a conceptually simple function $\zeta[R]$ that provides a satisfactory representation of the dynamical phenomena. If the channel structure was rigidly fixed in space during the simulations, the reaction coordinate function $\zeta[R]$ could be identified with the position of the ion along the axis of the channel. Such a simplification was possible in the previous study of a periodic β-helix,[7] even though it was flexible. To introduce the full flexibility of the channel, the reaction coordinate of the system must be properly defined as a relative coordinate of the ion with respect to the channel. One simple choice that exploits the symmetry of the gramicidin dimer is to define the reaction coordinate ζ as the projection of the ion position onto the vector joining the centers of mass of the gramicidin monomers; that is,

$$\zeta[R] \equiv \mathbf{u}\cdot(r_{\text{ion}} - R_{\text{CM}}) \tag{2}$$

where r_{ion} is the position of the ion, R_{CM} is the center of mass of the full dimer, and $\mathbf{u}$ is a unit vector calculated from the center of mass of the two monomers, R_{CM}^1 and R_{CM}^2,

$$\mathbf{u} = \frac{(R_{\text{CM}}^1 - R_{\text{CM}}^2)}{\|R_{\text{CM}}^1 - R_{\text{CM}}^2\|} \tag{3}$$

This straight-line path for doing perturbation calculations is convenient and gives the correct potential of mean force along that path (see below). Use of it as the reaction path is somewhat arbitrary. However, the rate constant resulting from the reactive flux formalism, which includes the transmission coefficient, is independent of that choice.[23] Furthermore, even though the reaction coordinate chosen here is a straight line, any curvature in the path of the ion (e.g., a helical path) is accounted for by the fluctuations of the system during the configurational sampling.[8] If large deviations from the straight-line path were important, they would lead to a small value for the transmission coefficient.

A formal definition of the reaction coordinate function $\zeta[R]$ is necessary to obtain meaningful averaging in eq 1. This problem has not been fully recognized in previous calculations of the free energy profile, in which the reaction coordinate remained unspecified.[24-26] In such studies, the free energy profile is blurred by a convolution with the uncertainty in the reaction coordinate. Our choice of reaction coordinate preserves the full internal flexibility of the channel and satisfies ones physical intuition about the permeation process. It is consistent with the formally correct statistical mechanical average in eq 1.

During the molecular dynamics simulations, the center of mass of the dimer is kept fixed at the origin and the channel $\mathbf{u}$-axis is oriented along the x-axis to maintain the position of the channel relative to the finite cylindrical aqueous system and the model membrane. This is done by resetting the position and orientation of the channel at each time step (see below). With these constraints, which are implemented in a consistent manner with eq 1, the unit vector $\mathbf{u}$ in eq 3 is parallel to the x-axis and the reaction coordinate $\zeta[R]$ is equal to the position of the ion along the x-axis. For the sake of simplicity, the reaction coordinate ζ will be referred to as x in the following, although it should be clear that this is true only in the constrained channel system.

The free energy profile is calculated using the free energy difference simulation technique.[7,27-29] Equation 1 can be expressed in a simpler notation by writing $W(x)$ in terms of a reduced configuration integral over all degrees of freedom $\bar{R}$ in the system other than x; that is,

$$e^{-[W(x)-W(x_0)]/k_BT} = \frac{\int d\bar{R}\, e^{-U(\bar{R};x)/k_BT}}{\int d\bar{R}\, e^{-U(\bar{R};x_0)/k_BT}} \tag{4}$$

where $U(\bar{R};x)$ represents the potential energy of the system with the reaction coordinate equal to x. From eq 4, the potential of mean force at a position $x + \Delta x$, $W(x+\Delta x)$, relative to that at x, $W(x)$, is

$$\Delta W(x \rightarrow x+\Delta x) = W(x+\Delta x) - W(x) \tag{5}$$

where the additive constant $W(x_0)$ cancels out in the free energy difference. The bracket with subscript x represents a statistical average over all degrees of freedom other than x (i.e., the coordinates of solvent and channel atoms, as well as the y and z coordinates of the Na^+) with the reaction coordinate held fixed at x; that is,

$$(e^{-\Delta U/k_BT})(x) = \frac{\int d\bar{R}\, e^{-\Delta U/k_BT} e^{-U(\bar{R};x)/k_BT}}{\int d\bar{R}\, e^{-U(\bar{R};x)/k_BT}} \tag{6}$$

and ΔU is the change in potential energy obtained by displacing the reaction coordinate from x to $x+\Delta x$ (i.e., ΔU is equal to $U(\bar{R};x+\Delta x) - U(\bar{R};x)$). From eq 5 it follows that a series of free energy differences in the neighborhood of the point x at which the simulation is performed can be evaluated from the single trajectory as long as Δx is not too large. The full profile is constructed by adding together the free energy differences obtained with eq 5 at the points x_n; that is,

$$W(x_{n+1}) = W(x_n) + \Delta W(x_n \rightarrow x_n+\Delta x) = \sum_{i=1}^{n} \Delta W(x_i \rightarrow x_i+\Delta x) - \Delta W(x_{i+1} \rightarrow x_{i+1}-\Delta x) \tag{7}$$

where Δx is the distance between two successive simulations (i.e., $\Delta x = |x_{n+1} - x_n|$).

The free energy profile can also be calculated by integrating the reversible work done by the mean force $\langle F(x)\rangle$ acting on the ion in the x direction,[7]

$$\Delta W(x \rightarrow x+\Delta x) = \int_x^{x+\Delta x} \langle F(x')\rangle\, dx' \tag{8}$$

where the trapezoidal rule is used to evaluate the integral in the present application. One advantage of this formulation is that the mean force can be decomposed linearly into a sum of contributions α (e.g., from solvent, channel, etc.)

$$\langle F(x)\rangle = \sum_\alpha \langle F_\alpha(x)\rangle \tag{9}$$

This allows the decomposition of the free energy profile $\Delta W(x+\Delta x)$ into a sum of contributions

$$W(x+\Delta x) = \sum_\alpha W_\alpha(x+\Delta x) \tag{10}$$

This approach, which is analogous to thermodynamic integration, is used here to analyze the long-range electrostatic contributions from the distant water molecules.

The present calculations are based on the perturbation of the free energy of the system with respect to a small change in the position of the ion. This is similar in spirit to the umbrella sampling method used by Jordan[24] but is somewhat more straightforward because the ion has a fixed value of the reaction coordinate for each simulation. Other calculations have used an approach that consists of materializing the ion from nothing or a water molecule at successive positions along the channel axis.[25,26] This method constructs the free energy profile by assembling successive large numbers, each with a considerable statistical uncertainty. The total free energy of materializing a Na^+ ion is about 100 kcal/mol in bulk water, and it is on the same order in the channel. The statistical error of the free energy of materialization for long simulations (50 ps) is on the order of 5 kcal/mol,[30] which is of the same magnitude as the variation of the energy along the reaction coordinate. Moreover, the reaction coordinate x must remain constrained during the materialization to obtain meaningful statistical averages (see above), a condition that was not fulfilled in the calculations of Åqvist and Warshel.[25] It appears that their calculation would not converge to a well-defined value if the simulation length, τ, was increased arbitrarily; since no constraints were applied in the water to ion simulation, the ion could be anywhere in the limit $\tau \rightarrow \infty$. Moreover, a combination of free energy calculation and energy minimization techniques was used, so that the quantitative validity of their calculations is not clear. The present calculations, with the appropriate constraints, would converge to a unique result in the limit $\tau \rightarrow \infty$.

Computational Details and Simulation Procedure. To obtain averages that converge in a reasonable time in eq 6, the reaction coordinate

(23) Chandler, D. *J. Chem. Phys.* **1978**, *68*, 2959.
(24) Jordan, P. C. In Transport through membranes: Carriers, channels and pumps; Pullman, A., et al., Eds.; Kluwer Academic Publisher: Dordrecht, The Netherlands, 1988; p 237.
(25) Åqvist, J.; Warshel, A. *Biophys. J.* **1989**, *56*, 171.
(26) Mackay, D. H.; Edelsten, P. M.; Wilson, K. R. Unpublished results described in: Jordan, P. C. *J. Phys. Chem.* **1987**, *91*, 6582.
(27) Zwanzig, R. W. *J. Chem. Phys.* **1954**, *22*, 1420.
(28) Tobias, D. J.; Brooks, C. B., III. *Chem. Phys. Lett.* **1987**, *142*, 472.
(29) Paci, E.; Ciccotti, G.; Ferrario, M.; Kapral, R. *Chem. Phys. Lett.* **1991**, *176*, 581.
(30) Tidor, B. Unpublished results.

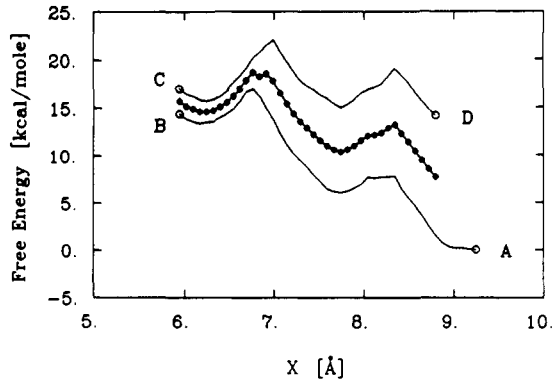

Figure 2. Free energy profile in the entrance region, I (solid line), calculated with a series of trajectories by moving the Na^+ ion from point A (x = 9.17 Å) to point B (x = 6.02 Å) and then backward from point C to point D (x = 8.72 Å); the simulation results were extrapolated beyond the end points to yield the values shown in the figure (see text). The best estimate (circles) was obtained by double sampling, combining the configurations of the two series of trajectories (A to B and C to D). The various profiles have been offset vertically for a clearer display; in reality B and C coincide (see also Figure 1).

increment Δx in eq 5 must be sufficiently small so that the ensemble of configurations with the ion constrained at x has a significant overlap with that with the ion constrained at $x \pm \Delta x$. Clearly, it is also desirable to choose Δx as large as possible to minimize the total number of simulations necessary to cover a significant distance along the reaction coordinate. By a series of trial calculations, a distance Δx = 0.075 Å was found to be a satisfactory compromise. After an equilibration of 10 ps with the ion at the initial position, the simulation procedure is as follows: (i) A 5-ps trajectory is generated with the ion constrained at x and the free energy difference calculated for ±0.075 Å. (ii) To reach the position for the next simulation, the ion is displaced by 0.01 Å along the x axis 15 times, each time followed by 50 steps of molecular dynamics for a total displacement of 0.15 Å. (iii) The 9 water molecules inside the channel and those within 8 Å of the ion are heated to 600 K for 2 ps followed by 2 ps at 300 K to remove local strain around the ion. During the high-temperature portion of the annealing cycle, the channel atoms and the model membrane are kept fixed and harmonic constraints are applied to the 9 water molecules inside the channel to maintain the relative oxygen–oxygen distance of nearest neighbors in the neighborhood of 2.9 Å while homogenizing the water positions inside the channel. This was followed by 2 ps of dynamics with the constraints present. The full system is then equilibrated at 300 K for 3 ps without constraints. (iv) Go back to step i and repeat the cycle.

This procedure was applied n times to generate n molecular dynamics trajectories that provide the configurational sampling used to evaluate the free energy increments $\Delta W(x_n \rightarrow \pm\Delta x)$ in eq 6 along a path going from the initial position x_1 to the final position x_n. If the configurational sampling represented an unbiased evaluation of eq 6, the free energy profile calculated with eqs 5 and 7 would not depend on the history or the preparation of the system. Calculations indicated that there is significant hysteresis in the calculated free energy increments ΔW because the results depended on the order in which the series of n trajectories was generated; i.e., moving the ion forward from x_1 to x_n or backward from x_n to x_1 ($x_n = x_1 + 2n\Delta x$) led to different results. An example of such nonequilibrium hysteresis effects in the entrance region of the channel is shown in Figure 2, where the disagreement between the forward and backward calculation is about 10 kcal/mol in going backward from 8.8 to 6.0 Å and then forward from 6.0 to 8.8 Å. Hysteresis was also observed in studies of ion transport inside the simplified β-helix where the periodicity of the system made it possible to determine the magnitude of the hysteresis and correct for it in a straightforward fashion.[7] An average hysteresis of +0.55 kcal/(mol Å) was observed for Na^+ in the periodic β-helix calculations when a 30-ps simulation was used at each value of x (the equilibration period was 5 ps and the production period was 25 ps).[7] In that calculation it was demonstrated that equilibration rather than the statistical error in the averages was the major problem. Similar sampling bias has been observed in free energy calculations of solutes in bulk water.[31] The problem is more severe in the highly confined channel system than in bulk solution due to the slower relaxation of the water molecules. The lack of equilibration is particularly critical at the entrance of the channel where the relaxation of the water molecules is slower than that in the bulk or in the interior of the channel.[13] The two slow processes causing problems in this region involve the ion–ethanolamine contact and the water–backbone contacts at the entrance. Test calculations with an equilibration period increased from 5 to 15 ps did not lead to more complete relaxation of the configurations, since the ΔW values were unchanged. This indicates that much longer trajectories are required. Unfortunately, the size of the present system and the resulting cost in computer time prevented the use of significantly longer equilibration periods. To extract the best estimate of the free energy profile with the available computer time, special care was given to the nonequilibrium hysteresis problem in each of the three regions that were studied. The magnitude of the hysteresis can be estimated by using a complete thermodynamic cycle; i.e., calculating $W(x)$ with two series of simulations, one going successively from x_1 to $x_1 + 2n\Delta x$, and the other going backward from $x_1 + 2n\Delta x$ to x_1. Since the two profiles should be identical according to eq 4, any disagreement between them is an indication of hysteresis due to insufficient equilibration, if the statistical error is small and random. The best estimate of the free energy profile from the results is obtained by averaging the information from the two series of calculations; that is, the free energy increment for each position x_1 is determined from eq 6 by using the configurations of the forward and backward series; i.e.,

$$e^{-\beta\Delta W_{best}} = {}^1/_2[e^{-\beta\Delta W_{forward}} + e^{\beta\Delta W_{backward}}]$$

No electrostatic "image" charge interactions or hydrocarbon polarization was added to the free energy profile calculated from the finite cylindrical system used in the simulations. It is shown in Appendix A that continuum electrostatic considerations indicate that the effect on the free energy from the finite nature of the cylindrical system is comparable in the aqueous phase and in the pore region so that no correction is necessary. This contradicts the conclusions reached by others about the importance of hydrocarbon polarization effects.[24,25]

Constraints. As outlined above, it is necessary to introduce constraints to maintain the relative position and orientation of the channel with respect to the finite cylindrical simulation system. Each dynamics step is done without constraints. After each step, the dimer is first translated to bring its center of mass back to the origin and then reoriented to align the center of mass of each monomer with the axis of the fixed cylindrical system corresponding to the boundary potential and the positions of the images. To reorient the dimer, the formula for infinitesimal rotations is applied to the coordinates x_i,y_i,z_i of all channel atoms

$$x_i \rightarrow x_i$$

$$y_i \rightarrow y_i - x_i\left[\frac{Y_{CM}{}^1}{X_{CM}{}^1}\right] \qquad z_i \rightarrow z_i - x_i\left[\frac{Z_{CM}{}^1}{X_{CM}{}^1}\right] \qquad (11)$$

where $X_{CM}{}^1, Y_{CM}{}^1, Z_{CM}{}^1$ represents the position of the center of mass of the first monomer. To constrain the reaction coordinate in a way consistent with eq 2, the x coordinate of the ion is fixed. The equilibrium average represents the integration over all other degrees of freedom in the system, including all internal flexibility of the channel and the motion of the ion in the cross section perpendicular to the x-axis. This implementation of the constraints is consistent with the Verlet algorithm used to compute the trajectories; it is similar in spirit to the SHAKE algorithm.[32]

Free Energy Calculations. The dimer channel extends from x = −10 Å to x = +10 Å with its center of mass located at the origin. Free energy calculations were performed in the three regions that are expected to differ most from a periodic β-helix: (I) the transition from bulk-like solvation of the ion to single file, (II) the single-file region at the entrance of the channel, and (III) the intermonomer junction at the center of the dimer channel.

Region I: Beginning of Single File (See Figure 2). The initial system was equilibrated for 10 ps after replacing a water molecule located at x = 9.25 Å by a Na^+ ion. The free energy increments ΔW were calculated using the procedure described with 21 successive simulations, moving the ion from 9.17 to 6.02 Å. A second series of 17 trajectories was generated moving the ion back from 6.17 to 8.72 Å. The configurations of the two series of trajectories were combined to average out the hysteresis bias in calculating the free energy increments in eq 6. The results are shown in Figure 2. A simulation was first made from A to B; B and C in the figure are the same point but they are displayed to make the results clearer; the

(31) Mazor, M.; Pettitt, M. B. *Mol. Simul.* **1991**, *6*, 1.

(32) van Gunsteren, W. F.; Berendsen, H. J. C. *Mol. Phys.* **1977**, *34*, 1311.

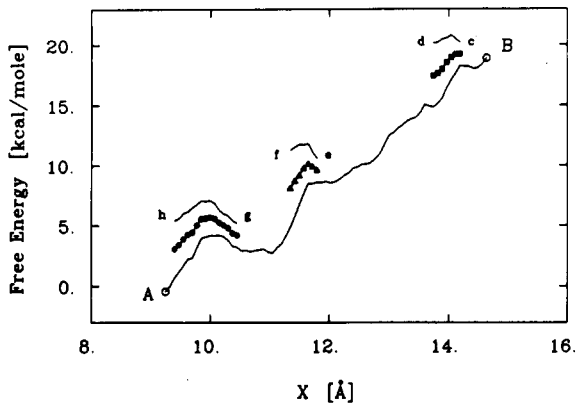

Figure 3. Free energy profile in the single file to the bulk transition (region II), calculated with one series of trajectories (solid line) by moving the Na^+ ion from x = 9.17 Å (point A) to x = 14.95 Å (point B). Three segments generated from c to d (14.12 to 13.82 Å), e to f (11.72 to 11.42 Å), and g to h (10.37 to 9.47 Å) show discrepancies due to the nonequilibrium hysteresis. The best estimates were calculated using all the configurations available by double sampling (squares, triangles, and circles). The various profiles have been offset vertically for a clearer display (see also Figure 1).

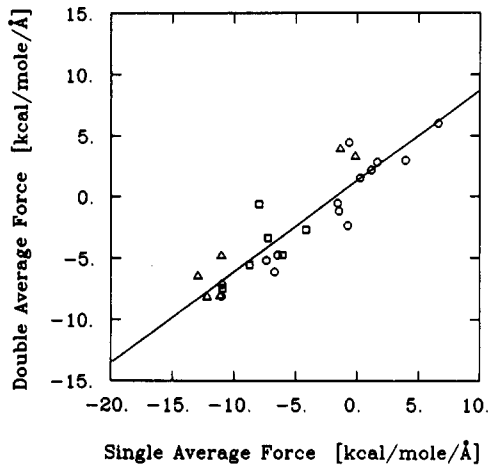

Figure 4. Comparison of the biased forces $\langle F\rangle_b$ with the best estimates of the forces calculated at three locations identified with squares, triangles, and circles, as in Figure 3. The best fit to $\langle F\rangle_u \approx A\langle F\rangle_b + B$ (eq 12) gives A = 0.7423 and B = 1.3222 kcal/(mole Å).

second simulation was done from C to D, where the value is different from A due to hysteresis. All values are relative as is evident from eq 1.

Region II: Single File to Bulk Water Transition (See Figures 3, 4, and 5). A series of 36 trajectories was generated by moving the ion successively from 9.17 to 14.57 Å, starting from the initial equilibrated structure used for region I of the profile. In view of the larger distance to be covered, a full backward computation was not attempted. Instead, nonequilibrium effects were probed over three shorter stretches: 7 trajectories were calculated from 10.37 to 9.47 Å, 3 trajectories from 11.72 to 11.42 Å, and 3 trajectories from 14.12 to 13.82 Å. A best estimate for the three stretches was calculated by combining the configurations of the forward and backward series of trajectories. The results are shown in Figure 3.

To obtain a correction for the nonequilibrium effects over the entire region, the average forces $\langle F(x)\rangle$ were examined at each calculated point along the reaction coordinate. In Figure 4 the biased forces $\langle F\rangle_b$ calculated from the forward series of simulations are compared with the estimates of the forces calculated by averaging the $\langle F(x)\rangle$ obtained from the forward and backward simulations in the three stretches where both were done. An approximate linear relation

$$\langle F\rangle_u \approx A\langle F\rangle_b + B \tag{12}$$

is observed between the biased forces, $\langle F\rangle_b$ (forward), and the unbiased forces, $\langle F\rangle_u$ (forward and backward). The values of the coefficients A and B in eq 12 were calculated by least-squares fitting; they are A = 0.7423 and B = 1.3222 kcal/(mole Å), respectively. Assuming that the linear relation is valid over the whole of region II, it is possible to use eq 12 to correct the free energy profile obtained by the forward series of simulations. The unbiased profile $W_u(x)$ is obtained by integrating the average unbiased force from x_1 = 9.17 Å to the position x; i.e.,

$$W_u(x) \cong AW_b(x) - B(x-x_1) \tag{13}$$

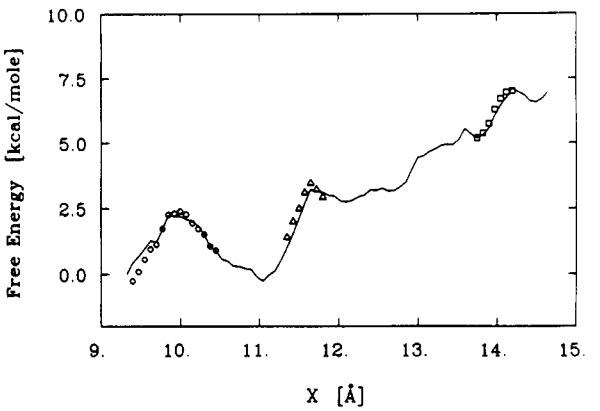

Figure 5. Free energy profile in region II after linear scaling with eq 13 to correct the nonequilibrium hysteresis (solid line) shown with the best estimate calculated at three locations identified with squares, triangles, and circles, as in Figure 3 (see also Figure 1).

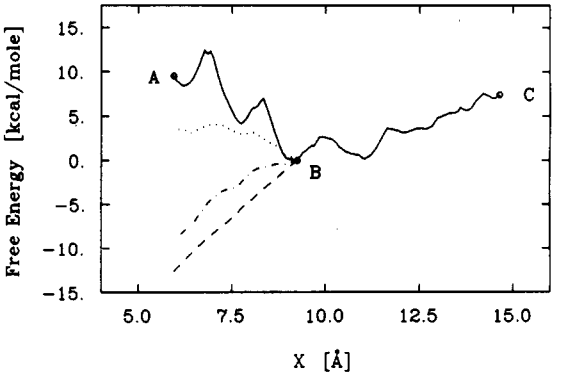

Figure 6. Free energy profile in the entrance region (solid line) including the transition from bulk to single file after hysteresis correction with double sampling (region I, A to B) and average force scaling (region II, B to C). The attractive mean force contributions of the all the water molecules excluding the two nearest neighbors in the single-file region are shown (dot-dashed line) and decomposed into the contribution of the water inside the channel (dashed line) and the bulk water (dotted line).

The comparison between the corrected profile and the best estimate, calculated from the forward and backward series, is shown in Figure 5. The agreement is satisfactory. The best estimate of the free energy profile for the whole entrance region (I and II) is shown in Figure 6, which was obtained by simply connecting the two sets of results, which are relative to the arbitrary zero at 9.17 Å.

Region III: Intermonomer Junction (See Figure 7). The initial system was equilibrated for 5 ps after replacing a water molecule located at x = −1.05 Å by a Na^+ ion. The profile was calculated by moving the ion from −1.05 to +1.05 Å with 14 simulations displaced symmetrically with respect to the x-axis. The symmetry of the dimer channel is such that statistical averages obtained with the ion at $+x$ should be equivalent, after a two-fold rotation about an axis through the center, to those obtained for the ion at $-x$. In particular, $W(x) = W(-x)$. Deviations of the free energy profile from this symmetry are due to incomplete sampling. Consequently, the expected symmetry of the profile was exploited to improve the statistical average of eq 6 by combining the configurations on both sides of the x-axis. The profile was extended from 1.05 to 1.95 Å with six simulations to determine the behavior in the interior of the monomer at the energy minimum located at 1.65 Å, so that the present results could be correlated with those of the periodic β-helix simulation. The results are shown in Figure 7.

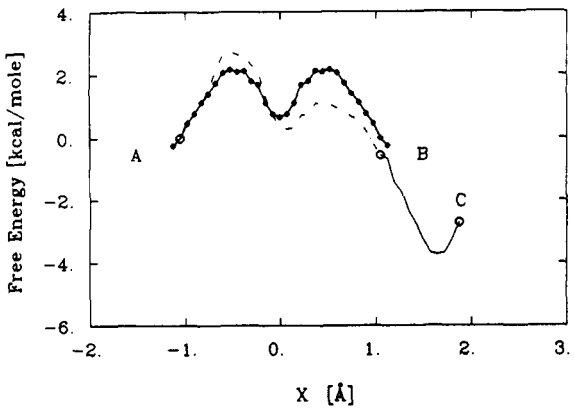

Figure 7. Free energy profile in the intermonomer (region III), calculated with one series of trajectories (dot-dashed line) by moving the Na^+ ion from $x = 1.05$ Å (point A) to $x = -1.80$ Å (point B). The best estimate between +1.05 and −1.05 Å (circles) was obtained by exploiting the symmetry of the free energy profile of the dimer.

Results and Analysis

The results obtained in all of the simulations are summarized in Appendix B. Here we describe them and their significance.

Free Energy Profiles. The free energy profiles at the channel entrance (region I), the single file to bulk water transition (region II), and the intermonomer junction (region III) are shown in Figures 6 and 7; Figure 1 shows their relation to the channel model. The effects of nonequilibrium hysteresis can be observed in all three regions. In regions I and II the insufficient equilibration creates an effective repulsive force pointing in the direction opposite to the sequence of free energy simulations. In particular, at the entrance (region I and II), a significant disagreement is observed between the results obtained from the forward and backward series of trajectories. Considering the free energy profile in the region shown in Figure 2, the energy difference between point $x = 8.72$ Å and $x = 6.02$ Å is 14 kcal/mol along path A to B while it is 2.5 kcal/mol along path C to D. Thus, the disagreement between the two paths (the hysteresis) is on the order of 11 kcal/mol. The best that can be done is to combine the configurations of all the trajectories available for each value of x. The free energy difference between $x = 6.02$ Å and $x = 8.72$ Å that results from combining the two series of calculations is 7.5 kcal/mol. In region II at the bulk interface (see Figures 3, 4, and 5), insufficient equilibration again leads also to an effective repulsive-like force biasing the free energy profile. Assuming that the biasing is uniform over the whole of region II, the calculated profile was corrected with the empirical linear relation eqs 12 and 13. In region III at the junction between the two monomers (see Figure 7), insufficient equilibration results in a loss of symmetry in the free energy profile. In this region the bias does not correspond to an effective repulsive-like force and a best estimate of the free energy profile is obtained by combining the information from the trajectories at $\pm x_n$ by virtue of the symmetry of the system.

Hysteresis effects are a measure of the minimum error present in the calculations;[31] i.e., the absence of an hysteresis is a necessary, but not sufficient, condition for the convergence of the free energy calculation. In spite of the considerable hysteresis, the salient features of the profile, such as the existence and location of the free energy wells and barriers, appear to be reliable, since they are generally reproduced in both the forward and backward series of calculations. Free energy minima are present in the three regions of the profile. The positions of the relative minima along the x-axis are 6.17, 7.67, 9.25, and 10.97 Å in regions I and II and 0.0 and 1.65 Å in region III. It is noteworthy that the position of these minima corresponds approximately to integer multiples of 1.55 Å ($n = 0, 1, 4, 5, 6, 7$), the length of the helical unit in the periodic β-helix studied previously.[7] This is reasonable, since the main-chain structure of the more realistic gramicidin dimer model used here is close to that of the periodic β-helix. The minima observed at 9.30 and 10.85 Å in the entrance region shown in Figure 6 have the lowest energy relative to the rest of the profile in this region and could correspond to the major Na^+ binding sites detected experimentally by NMR from ion-induced ^{13}C chemical shift.[11] X-ray diffraction studies of gramicidin yield a position 9.6 Å from the center for Tl^+.[33]

No sharp free energy barrier is observed at the entrance of the channel in the region from 15 to 10 Å, as the first ion hydration shell of the ion is transformed to the single-file aqueous solvation (see the radial distribution functions shown below). This is not surprising, since the solvation of the ion by the channel carbonyls is of the same order as that of the water they replace. The ab initio interaction energy of Na^+ with acetamide, used as a model of the carbonyl group, is 38 kcal/mol, and the interaction of Na^+ with water is 24 kcal/mol.[7,19] The highest activation barrier is observed at $x = 7$ Å. It is near the entrance of the channel but occurs after the single-file solvation has already formed. It is possible that the barrier is caused by electrostatic interactions of the ion with the water molecules in the bulk region. This would represent the microscopic analog of the "image charge" energy barriers observed in electrostatic calculations, in which the bulk water, the channel, and the membrane are modeled as continuous media with different dielectric constants.[34-36] In continuum electrostatics, the "image charge" energy barrier arises from the fact that the membrane region (low dielectric constant) provides a less favorable environment than the bulk water (high dielectric constant). To investigate the presence of continuum-like electrostatic effects in the molecular dynamics calculations, it is necessary to distinguish the roles played by the nearest and the most distant water molecules. In the channel the dominant forces acting on the ion involve the nearest ligands (two water molecules and four carbonyls). Continuum-like contributions can be identified with the forces arising from the water molecules that are not in direct contact with the ion (eight water molecules are in the channel and the others are in the bulk region). The free energy mean force decomposition method,[7] based on eqs 8 and 10, was used to calculate the contribution from the bulk and channel water molecules not directly in contact with the ion. The results, shown in Figure 6, clearly indicate that long-range electrostatic interactions have the opposite effect of that expected from the continuum electrostatic models. Attractive forces directed toward the inside of the channel result from the distant water molecules. Further decomposition reveals that the average force arising from the bulk region tends to attract the ion outside the channel as expected, but that this effect is more than compensated by the significant attractive forces arising from the electrostatic interactions with the eight water molecules pointing toward the ion inside the channel. Because the orientational freedom of the water molecules inside the channel differs from that of bulk water (i.e. they are all oriented in one direction),[50] a continuum electrostatic based on an isotropic dielectric constant does not account for the directionality induced by the pore environment. Since it does not arise from distant electrostatic effects, the entrance barrier must be due to local interactions involving the ion, the two nearest water molecules, and the channel. Thermodynamic decomposition of the free energy profile of Na^+ in the periodic β-helix into enthalpic and entropic contributions indicated that the free energy barrier was controlled by the water–peptide and peptide–peptide hydrogen bond interactions.[7] Such analysis is not possible with the short trajectories used in the present study because the enthalpic and entropic contributions are much more difficult to evaluate accurately due to the large

(33) Olah, G. A.; Huang, H. W.; Liu, W.; Wu, Y. *J. Mol. Biol.* **1991**, *218*, 847.
(34) Parsegian, A. *Nature* **1969**, *221*, 844.
(35) Jordan, P. C. *Biophys. Chem.* **1981**, *13*, 20.
(36) Jordan, P. C. *J. Membr. Biol.* **1984**, *78*, 91.

fluctuations in the total energy of the system. Further work will be necessary to see if the same contributions are important at the entrance of the dimer channel. The effect of the ethanolamine will also have to be considered.

The location of the entry barrier at $x = 7$ Å may appear to be inconsistent with the experimental observation that the entry step is not very sensitive to the membrane potential.[37] Since the electric field due to the transmembrane voltage is expected to be negligible except inside the channel,[38] it is usually concluded that the rate-limiting step for the permeation process must be located outside the single-file region, which is between 10 and −10 Å. This argument is based on Eyring rate theory models fitted to the data;[38] i.e., the sublinear current–voltage characteristics at low permeant-ion concentrations are interpreted as an indication that the kinetics of ions entering the channel are rate-limiting and are not sensitive to the applied potential. This implies that they must be located outside the single-file region. The underlying assumption leading to this conclusion is that the total energy profile acting on the ion in the channel in presence of the membrane potential is

$$W(x;V) \cong W(x;0) + \frac{qVx}{L} \qquad (14)$$

It has been shown that eq 14 is incorrect,[7,8] even to lowest order in the membrane potential. The free energy profile of an ion in the presence of an applied voltage, $W(x;V)$, should also include the effect of the electric field on the charges associated with the channel. The correct expression leads to a modified free energy profile of the form

$$W(x;V) \cong W(x;0) + \frac{qV}{L}\left[x + \frac{\langle \Delta\mu(x) \rangle}{q}\right] \qquad (15)$$

where $W(x;0)$ is the free energy profile in the absence of the membrane potential and $\langle \Delta\mu(x) \rangle$ is the change in the average dipole of the system, including channel and water atoms, as the ion moves along the x-axis. The quantity $x + \langle \Delta\mu(x) \rangle / q$ is called the "electric distance".[2] The change in the dipole induced by Na^+ was estimated for a periodic β-helix and was shown to be significant.[7] Since an estimate of $\langle \Delta\mu(x) \rangle$ requires simulations longer than the 5 ps used here, it is possible only to make qualitative arguments for the effect of the dipole of the system during the permeation process. It is observed in the simulations that the internal water molecules are pointing toward the ion in the interior of the channel. This implies that 9–10 water molecules are oriented approximately in the $+x$ direction when the ion is located at $x = +10$ Å and that the same water molecules are pointing in the $-x$ direction when the ion has crossed the channel. From the value of the dipole moment of a water molecule in bulk liquid (0.5 e Å),[15] this process would correspond to a total dipole change of 5 e Å during the complete translocation of an ion. Therefore, the observed "electric distance" and the actual structural distance traveled by an ion across the gramicidin channel may be estimated by eq 15 to differ by about 5 Å due to the orientation of the water molecules. The water molecules at the mouths of the channel also have anisotropic orientations[13] and could contribute to changes in the dipole induced by the ion. Other effects such as the nonequilibrium reorganization of the interfacial polarization[38] and the counterion depletion at the channel mouth[39] may influence the observed voltage dependence of the transport rate through the gramicidin channel. Since most of the analysis of experimental flux data was based on specific assumptions concerning the number of barriers (three sites, two barriers), many neglected interfacial polarizations, and all neglected dipole distortions, its conclusions are uncertain. The present observations provide a qualitative microscopic picture that can help in the construction of phenomenological models to fit the experimental flux data.

(37) Andersen, O. S. *Biophys. J.* **1983**, *41*, 119.
(38) Andersen, O. S. *Biophys. J.* **1983**, *41*, 135.
(39) Peskoff, A.; Bers, D. M. *Biophys. J.* **1988**, *53*, 863.

Table I. Position of the Free Energy Minima in the Dimer Channel

minima	residues[a]				position x (Å)
0	L-Val1′	L-Ala3	L-Ala3′	L-Val1	0.00
1	formyl	L-Ala5	L-Val1′	L-Ala3	1.65
2[b]	Gly2	L-Ala7	formyl	L-Ala5	3.10
3[b]	D-Leu4	L-Trp9	Gly2	L-Ala7	4.65
4	D-Val6	L-Trp11	D-Leu4	L-Trp9	6.17
5	D-Val8	L-Trp13	D-Val6	L-Trp11	7.67
6[c]	D-Leu10	L-Trp15	D-Val8	L-Trp13	9.25
7[c]	D-Leu12	ethanol	D-Leu10	L-Trp15	10.97

[a] Primed residue numbers belong to the second monomer (see also Figure 9). [b] Predicted from the periodic β-helix. [c] Lowest free energy minima and probably the major Na^+ binding sites.

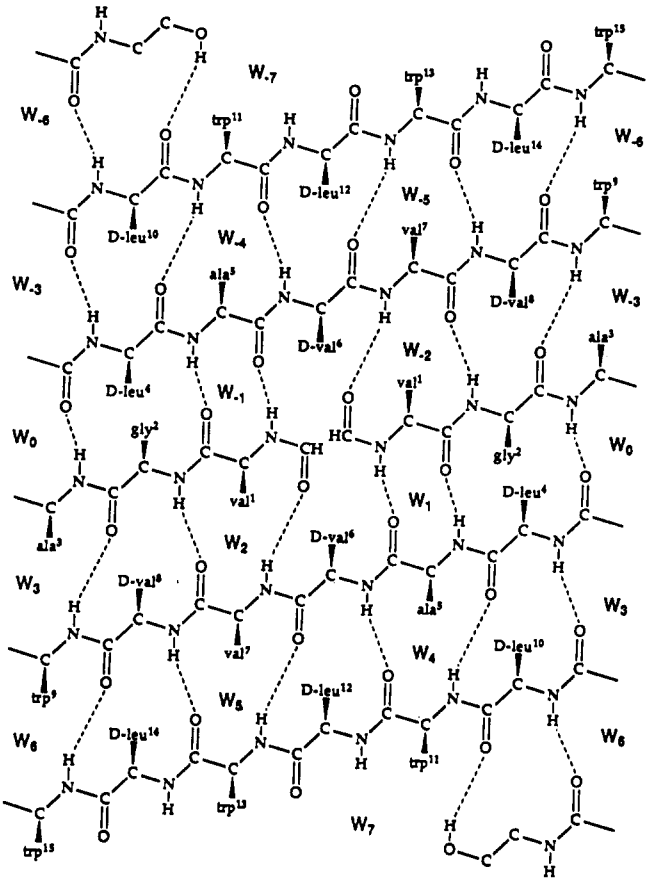

Figure 8. Schematic representation of the right-handed dimer to indicate the presence of the seven energy wells in the free profile. In each of the identified wells, the Na^+ ion makes contact with the four nearest carbonyl oxygens, for example with 8, 13, 6, and 11 in well W_5. The major binding sites are W_6 and W_7. See also Table I.

Structural Aspects. In all the free energy minima observed in the profiles shown in Figures 6 and 7, the Na^+ ion interacts closely with four carbonyl oxygens and two water molecules. The only exception is the minimum located at $x = 10.97$ Å (region II), where the ion interacts with three carbonyl oxygens, three water molecules, and the OH of the ethanolamine tail. The carbonyl oxygens making specific contact with the ion are listed in Table I and are illustrated schematically in Figure 8. Similar contacts with the four nearest carbonyl oxygens along the channel axis were observed in the study of the free energy profile along the periodic β-helix.[7] We generalize this observation to the rest of the channel and assume that there are two free energy minima at 3.10 and 4.65 Å (minima 2 and 3). These minima are indicated in Table I and in Figure 8. Even though the solvation structure around the Na^+ ion in the last well at $x = 10.97$ Å is not identical to the one found in the single-file region (only three carbonyl oxygens are nearest neighbors), the position of the well is consistent with the periodicity of the β-helix.

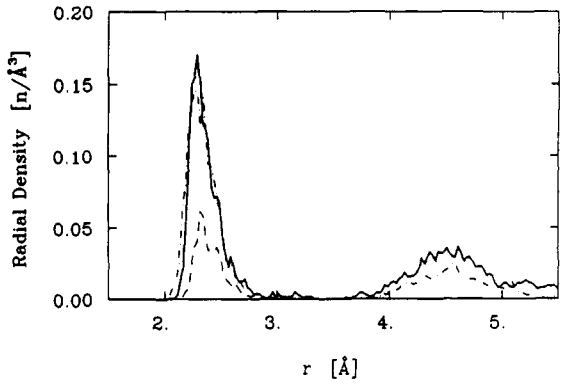

Figure 9. Radial density distribution function of water (solid line), carbonyl oxygen (dot-dashed line), and ethanolamine tail (dashed line) around the Na^+ ion at x = 10.97 Å (in the region of the outer binding site (minimum 7 in Table I)). The Na^+ ion is surrounded on the average by three water molecules and three carbonyl oxygens (D-Leu12, D-Leu10, and L-Trp15). The carbonyl oxygen peak is slightly closer to the ion than the water oxygen peak.

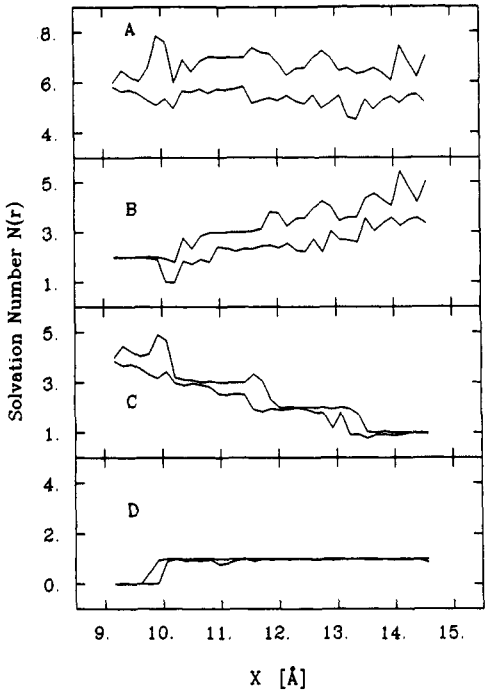

Figure 10. Average number of nearest neighbor ligands around the Na^+ ion during the transition from single-file solvation (at x = 9.17 Å) to quasi-bulk solvation (at x = 14.95 Å). The oxygens from water (B), carbonyl (C), and ethanolamine tail (D) and the total (A) number of ligands are shown. The upper line represents the average number of neighbors of the Na^+ ion inside a sphere of radius 3.5 Å, and the lower line, the average number inside a sphere of radius 2.5 Å. At x = 14.5 Å, the ion is making contact with carbonyl oxygen D-Leu14.

The progressive transformation of the solvation from the bulk-like solvation to the single-file region is best described in terms of the radial distribution functions for the Na^+ ion. The radial density distribution of the main interacting partners around the Na^+ ion in the outer binding site (i.e., water oxygen, carbonyl oxygen, and ethanol oxygen) is shown in Figure 9. In this site, solvation by carbonyls is as important as solvation by waters. The number of nearest interacting partners found within a distance of less than 2.5 Å (lower line) or 3.5 Å (upper line) from the Na^+ ion during the transition from bulk-like to single-file solvation is shown in Figure 10. The radial distribution functions $g(r)$ of water oxygens around the Na^+ ion are shown in Figure 11. The statistical fluctuations in the radial distributions and in the average nearest neighbors reflect the limited configurational sampling

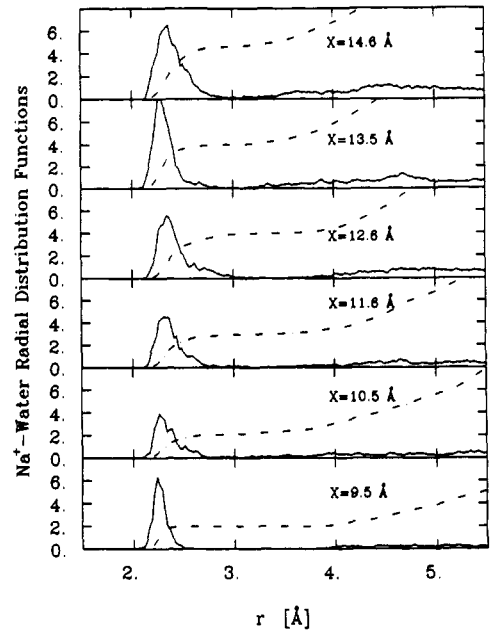

Figure 11. Radial distribution function of water oxygen $g(r)$ (solid line) and running hydration number $N(r)$ (dot-dashed line) around the Na^+ ion during the transition from single-file to bulk solvation.

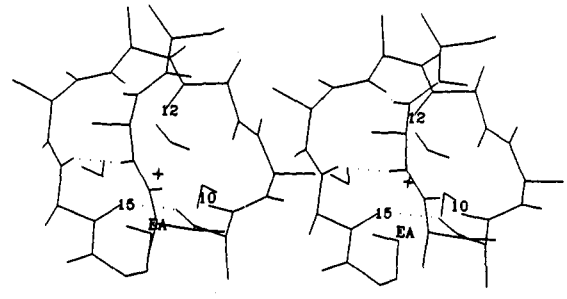

Figure 12. Stereo picture of the Na^+ ion in the outer binding site (energy minimum number 7) with the three nearest water molecules and the last residues of the monomer, including the ethanolamine tail. There are seven neighbors in the first solvation shell of the Na^+ ion.

with a 5-ps trajectory. The change in the structure involved in the solvation of the Na^+ takes place over a distance of 5–6 Å. At the farthest distance (14.95 Å), the Na^+ is still in contact with one carbonyl oxygen and the oxygen of the ethanolamine tail, which follows the ion. As the Na^+ ion leaves the channel, the interactions with carbonyl oxygens are lost in a step by step fashion; i.e., from four carbonyl contacts in the single-file region (x = 10 Å) to one in the quasi-bulk region at x = 14.95 Å, one carbonyl oxygen is lost about every 1.5 Å in accord with the helical periodicity. The increase in near-neighbor water molecules apparently does not follow a step by step mechanism. It is more characteristic of a continuous transformation from two waters in the single-file region to approximately four to five waters in the quasi-bulk region (in bulk water, Na^+ has five to six waters in the first hydration shell).[19] Contact with the ethanol is maintained over the whole transition region. At some stage the ethanolamine must lose contact with the Na^+ ion and be replaced by a water molecule, but this process was not observed during the simulations.

The looseness of the hydration shell surrounding the Na^+ ion is reflected by the difference in the number of nearest interaction partners closer than 2.5 and 3.5 Å. If the solvation shell was very rigid, the number of neighbors closer than 2.5 and 3.5 Å would be the same. The effects of the $1/r^4$ ion-induced dipole interactions in the empirical energy function are particularly important at these medium-range distances.[19] It is possible that the absence of this energy term would cause a large dehydration barrier; this has been observed in other calculations.[24,26] As the ion is losing

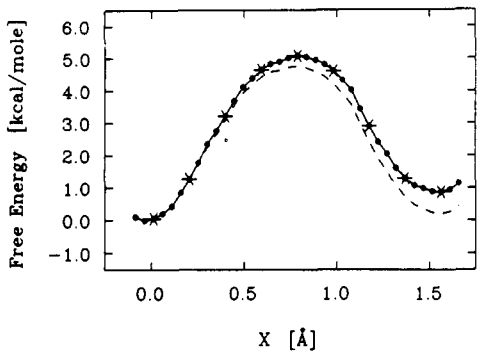

Figure 13. Free energy profile of the Na^+ ion along the axis of the periodic β-helix used in the construction of the midmonomer section for Figure 14. The solid line represents the calculated profile directly obtained from the perturbation technique. × indicates the locations of the nine simulations, and O represents the positions where free energy differences were computed. A hysteresis of 0.8 kcal/mol is observed. The linearly corrected profile is plotted with dashed lines.

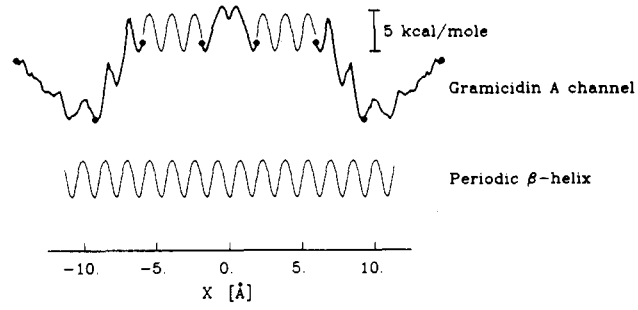

Figure 14. Free energy profile along the gramicidin dimer axis obtained by assembling the three regions considered in the present study (bold line) and a connector going from 6.02 to 1.65 Å (thin line) constructed from the free energy profile inside the periodic β-helix (shown at the bottom). The position of the connector was only adjusted vertically by addition of a constant energy term to the periodic free energy profile to match at x = 6.02 Å. Its amplitude was not scaled, and the horizontal position was neither adjusted nor scaled; i.e., the distance between the well of the period connector is 1.55 Å and the energy barriers are 4.5 kcal/mol, as calculated for the periodic β-helix. The vertical position of the intermonomer segment (region III) was adjusted such that the energy in the first wells located at ±1.55 Å is equal to the energy in the fourth wells located at ±6.02 Å. The lowest energy minima are located at ±9.27 and ±10.97 Å, corresponding to the Na^+ binding sites. The largest energy barrier is about 8 kcal/mol; it is in the entrance region between wells 5 and 4 located at ±6.95 Å.

water molecules, they are replaced by carbonyls that have a strong stabilizing interaction even at distances of 3–5 Å, when polarization is included. The polarization energy in the carbonyl–ion interaction leads to a minimum of 38 kcal/mol versus 32 kcal/mol for a pure Coulomb plus Lennard-Jones 6–12 term. Polarization effects in dehydration processes are presently being investigated in a simple model system.

Complete Free Energy Profile. The complete free energy profile of Na^+ and its interpretation is a major objective of theoretical descriptions of the gramicidin A channel. Although the present study is not able to provide this directly, it can be used to obtain an estimate of the essential aspects of the profile by combining the simulation results obtained here with those from the periodic β-helix.[7] This procedure is justified by the fact that the translocations in the midmonomer region and in the periodic β-helix are expected to be structurally and energetically very similar. In combining the two sets of results, we make use of the fact that the relative spacing of the energy minima of the β-helix profile matches that of the minima of the dimer profile in the entrance and at the intermonomer junction. The behavior of the energy barriers at the intermonomer junction differs somewhat from that at the β-helix, although there is a small well at x = 0.0 Å, where the β-helix has a normal minimum. Comparing the β-helix results and the present simulations (Figure 14), we see that, in terms of the position of the minima, there is an exact correspondence (including the midmonomer connector) without any distortion or scaling of any of the segments of the free energy profile.

To use a section of the profile of the periodic β-helix, it is necessary to find a correspondence with the segment calculated at the entrance (region I) and the segment calculated at the intermonomer junction (region III). The energy minima located at 1.65 and at 6.17 Å (i.e., minima number 1 and 4 in Table I) represent the limit of the midmonomer section. For the sake of simplicity, it is assumed that the free energy is the same in minima number 1 and 4. Using the calculated free energy profile of Na^+ in the periodic β-helix, shown in Figure 13, a "connector" of three barriers and two wells is constructed for the midmonomer section. The construction is shown in Figure 14 with the periodic profile of the β-helix drawn at the bottom of the figure. Such an approach is analogous to the matching done in the umbrella sampling method where different parts of a potential of mean force are connected by adding an arbitrary constant. One difference here is that the free energy profile in the middle section (the connector) comes from calculations done with a different system, the periodic β-helix. Nevertheless, the results provide an approximate description of the whole free energy profile of the gramicidin channel from the interior monomer contact to the almost-bulk-like region. The location of major binding sites and energy barriers will allow more accurate calculations to concentrate on these regions, which are rate-limiting for the transport.

Concluding Discussion

The free energy profile shown in Figure 14 is not a full theoretical prediction but an approximate construction based on the available simulation data. In spite of the considerable statistical uncertainty in the calculations, the general aspect of the profile is likely to be correct and should be useful for interpreting experimental data. There are 14 small energy barriers and 15 wells separated approximately by 1.5 Å, the helical unit of the periodic β-helix. It is apparent that the main features of the β-helix profile are reproduced in the dimer channel. Even through the dimer junction, the channel behaves almost like a single polypeptide β-helix and the free energy profile is only slightly perturbed. The positions of the binding sites located at the extremities of the channel also agree with the general aspect of the periodic pattern of the β-helix. The lowest energies relative to the rest of the profile are observed at 9.25 and 10.97 Å in the entrance region and correspond to the major Na^+ binding sites detected experimentally by NMR from ion-induced ^{13}C chemical shift.[40,41] The largest chemical shifts were observed for carbonyl carbon D-Trp11, L-Trp13, D-Leu14, and L-Trp15. In the binding sites the Na^+ ion is making contact with carbonyl D-Val8, D-Leu10, L-Trp13, L-Trp15, and two water molecules. At x = 14.5 Å, in the quasi-bulk region, the ion is making contact with carbonyl D-Leu14. The 9.25-Å site is in close accord with the Tl^+ position (9.6 Å) obtained from X-ray studies.[33]

There appears to be a larger activation barrier at the entrance in the single-file region, i.e., where the ion is surrounded by four carbonyl oxygens and two water molecules. Mean force decomposition shows that this barrier is caused by local interactions and is not due to long-range electrostatic forces. The barrier in the free energy calculation may be due, in part, to the channel constriction at the mouth. However, its magnitude could be exaggerated by nonequilibrium effects arising from the slower water relaxation at the channel entrance. No sharp free energy barrier is observed between 10 and 15 Å, as the first ion hydration

(40) Urry, D. W.; Prasad, K. U.; Trapane, T. L. *Proc. Natl. Acad. Sci. U.S.A.* **1982**, *79*, 390.
(41) Urry, D. W.; Walker, J. T.; Trapane, T. L. *J. Membr. Biol.* **1982**, *69*, 225.

Table II. Free Energy Perturbation Elements (kcal/mol): Region I[a]

x (Å)	forward $\Delta W(x-\Delta x)$ / $\Delta W(x+\Delta x)$	backward $\Delta W(x-\Delta x)$ / $\Delta W(x+\Delta x)$	average $\Delta W(x-\Delta x)$ / $\Delta W(x+\Delta x)$	x (Å)	forward $\Delta W(x-\Delta x)$ / $\Delta W(x+\Delta x)$	backward $\Delta W(x-\Delta x)$ / $\Delta W(x+\Delta x)$	average $\Delta W(x-\Delta x)$ / $\Delta W(x+\Delta x)$
6.02	0.543			7.67	0.285	0.564	0.408
	−0.250				−0.106	−0.362	−0.248
6.17	0.213	0.363	0.283	7.82	−0.136	−0.355	−0.256
	0.145	−0.099	0.011		0.287	0.525	0.394
6.32	−0.046	−0.160	−0.106	7.97	−0.432	−0.661	−0.557
	0.411	0.232	0.315		0.748	0.352	0.518
6.47	−0.326	−0.569	−0.459	8.12	0.095	−0.213	−0.079
	0.543	0.855	0.679		0.097	0.352	0.211
6.62	−0.791	−0.698	−0.746	8.27	−0.041	−0.769	−0.510
	1.013	0.798	0.896		0.063	0.850	0.335
6.77	−0.242	−1.114	−0.825	8.42	1.267	0.690	0.911
	−0.826	0.617	−0.463		−0.958	−0.738	−0.858
6.92	1.245	−0.726	−0.334	8.57	0.852	1.121	0.971
	−1.126	0.555	−0.748		−1.066	−0.914	−0.995
7.07	1.381	1.241	1.307	8.72	1.106	0.780	0.921
	−1.173	−1.024	−1.103		−0.991	−0.638	−0.840
7.22	1.007	1.048	1.027	8.87	0.779		
	−0.682	−0.900	−0.801		−0.446		
7.37	0.707	0.600	0.651	9.02	0.141		
	−0.864	−0.423	−0.683		−0.003		
7.52	0.701	0.559	0.626	9.17	0.114		
	−0.737	−0.374	−0.583		−0.037		

[a] Δx equals 0.075 Å, i.e., half the distance between the simulations.

shell of the ion is transformed to fit the constraints of the single-file solvation. This result contradicts a "dogma" concerning the dehydration process. The absence of a free energy barrier may be related to the relatively delocalized nature of the transition from single-file to bulk solvation. The transformation of the nearest solvation neighbors around the Na^+ takes place progressively over a distance of about 5–6 Å. The ion-induced polarization of the carbonyl appears to compensate, in part, for the loss of favorable interactions of the Na^+ ion with water molecules. No large barrier is observed at the intermonomer junction.

We finish this section with a discussion of the limitations of the present results and the need for future work. The large hysteresis found in the calculations due to insufficient equilibration limits the quantitative interpretation of the activation barriers, particularly at the entrance where the configurational relaxation of the system appears to be slower. It is clear that 10 ps is too short a time to equilibrate and sample the configurations of the system. The average displacement imposed on the ion in the calculation of the free energy profile is 0.15 Å every 10 ps. This would correspond to a total translocation time of 1–2 ns, i.e. a time at least 1000 times faster than the actual movement of an ion through the gramicidin channel.[8] The very rapid exploration of the free energy surface induces nonequilibrium hysteresis, as was also observed in the studies of the periodic β-helix.[7] However, for that case, longer simulations could be done because the simplicity and the symmetry of the system made possible an accurate correction for hysteresis effects. The more complex nature of the present system limits the simulation time and prevents a quantitative correction for the hysteresis. As shown in Figure 2, the nonequilibrium hysteresis is most important at the channel entrance due to the slower relaxation of the water molecules. Longer simulations could provide a more accurate estimate of the free energy profile in the entrance region. Temperature jumps and annealing techniques could be used to accelerate the equilibration of the system and improve the conformational sampling.[42] It should be stressed, however, that an increased statistical accuracy over the complete free energy profile would require very large computational resources. Even the relatively short equilibration and simulation times that were used in the present study represent on the order of 300 Cray YMP hours. A large number of simulations at different values of x are necessary due to the small distance increment Δx (0.075 Å). Future work and more extensive calculations will focus on the significant regions of the profile. The present calculations suggest that the rate-limiting barrier is located inside the channel after the single file to bulk transition. Once an accurate determination of the activation energy and its origin has been made, activated dynamics trajectories will be used to determine the rate of transport of Na^+. The absolute free energy difference of Na^+ in the main binding site relative to bulk water will be calculated to estimate the equilibrium binding constant.[43]

Acknowledgment. Helpful conversations with O. S. Andersen and D. Busath are gratefully acknowledged. J. Straub and J. Roberts provided help with the figures. The calculations described here were done at the Pittsburgh Supercomputer Center and supported in part by a grant from the National Science Foundation. Ten picoseconds of simulation required about 3 h of CPU time on a single processor of the Cray YMP.

Appendix A. Continuum Electrostatic Considerations

Potential problems in the calculation of the free profile caused by the use of a cylinder of finite radius must be addressed. A simple picture based on continuum electrostatics is sufficient to estimate the loss of interaction energy due to the finite size of the system. For a spherical ion, the Born free energy of solvation,[44] $\Delta\mu$, has a very simple dependence on the ionic charge Q, the radius σ, and the solvent dielectric constant ϵ; i.e.,

$$\Delta\mu = \frac{Q^2}{2\sigma}\left(\frac{1}{\epsilon} - 1\right) \qquad \text{(A.1)}$$

It has been shown recently that the representation by a continuum electrostatic is a valid approximation for a microscopic ion in a polar solvent.[45] The Born radius σ was identified as the first peak in the solute–solvent radial distribution and was found to depend on the charge of the ion, as well as on the type of solvent in which it is immersed. This microscopic interpretation of the Born model of solvation implies that the radius is different when the ion is solvated by bulk water or when it is in the channel. With

(42) Kuharski, R. A.; Bader, J. S.; Chandler, D.; Sprik, M.; Klein, M. L.; Impey, R. W. *J. Chem. Phys.* **1988**, *89*, 3248.
(43) Hinton, J. F.; Fernandex, J. Q.; Shungu, D. C.; Whaley, W. L.; Koeppe, R. E.; Millet, F. S. *Biophys. J.* **1988**, *54*, 527.
(44) Born, M. *Z. Phys.* **1920**, *1*, 45.
(45) Roux, B.; Yu, H. A.; Karplus, M. *J. Phys. Chem.* **1990**, *94*, 4683.

Table III. Free Energy Perturbation Elements (kcal/mol): Region II[a]

x (Å)	forward $\Delta W(x-\Delta x)$ / $\Delta W(x+\Delta x)$	backward $\Delta W(x-\Delta x)$ / $\Delta W(x+\Delta x)$	average $\Delta W(x-\Delta x)$ / $\Delta W(x+\Delta x)$	scaled (eq 12) $\Delta W(x-\Delta x)$ / $\Delta W(x+\Delta x)$	x (Å)	forward $\Delta W(x-\Delta x)$ / $\Delta W(x+\Delta x)$	backward $\Delta W(x-\Delta x)$ / $\Delta W(x+\Delta x)$	average $\Delta W(x-\Delta x)$ / $\Delta W(x+\Delta x)$	scaled (eq 12) $\Delta W(x-\Delta x)$ / $\Delta W(x+\Delta x)$
9.17	0.114			0.184	12.17	−0.208			−0.056
	−0.037			−0.127		0.326			0.142
9.32	−0.432			0.221	12.32	−0.218			−0.063
	0.698			0.419		0.399			0.197
9.47	−0.485	−0.192	−0.356	−0.261	12.47	−0.096			0.028
	0.503	0.416	0.458	0.274		0.249			0.085
9.62	−0.553	−0.160	−0.389	−0.312	12.62	0.003			0.101
	0.058	0.324	0.176	−0.056		0.148			0.011
9.77	−0.826	−0.251	−0.606	−0.514	12.77	−0.323			−0.141
	0.822	0.339	0.533	0.511		0.392			0.192
9.92	−0.119	0.049	−0.041	0.011	12.92	−0.781			−0.480
	0.110	0.070	0.089	−0.018		0.757			0.463
10.07	0.019	0.226	0.114	0.113	13.07	−0.210			−0.057
	0.048	−0.563	−0.333	−0.064		0.363			0.170
10.22	0.124	0.313	0.211	0.191	13.22	−0.269			−0.100
	−0.294	−0.141	−0.222	−0.318		0.324			0.141
10.37	0.495	0.410	0.451	0.467	13.07	−0.301			−0.125
	−0.088	−0.231	−0.164	−0.165		0.505			0.276
10.52	0.306			0.326	13.22	−0.255			−0.090
	0.048			0.064		0.160			0.020
10.67	0.126			0.193	13.37	−0.183			−0.037
	0.115			−0.014		0.131			−0.002
10.82	−0.029			0.078	13.52	−0.405			−0.202
	0.085			−0.036		0.686			0.410
10.97	0.262			0.294	13.67	0.153			0.213
	−0.056			−0.141		−0.081			−0.159
11.12	−0.433			−0.223	13.82	−0.312	−0.063	−0.0201	−0.133
	0.348			0.159		0.456	0.269	0.355	0.239
11.27	−0.648			−0.382	13.97	−0.817	−0.083	−0.557	−0.508
	0.780			0.480		0.654	0.246	0.416	0.386
11.42	−0.832	−0.230	−0.604	−0.518	14.12	−0.544	0.347	−0.252	−0.305
	0.968	0.221	0.484	0.620		0.598	−0.236	0.046	0.345
11.57	−0.913	0.033	−0.610	−0.578	14.27	0.043			0.131
	0.826	0.104	0.362	0.514		−0.007			−0.105
11.72	−0.011	0.702	0.245	0.091	14.42	0.204			0.251
	0.101	−0.528	−0.293	−0.024		0.084			−0.037
11.87	0.022			0.115	14.57	−0.318			−0.137
	0.090			0.032		0.497			0.269
12.02	0.128			0.194					
	0.103			−0.023					

[a] Δx equals 0.075 Å, i.e., half the distance between the simulations.

Table IV. Free Energy Perturbation Elements (kcal/mol): Region III[a]

x (Å)	forward $\Delta W(x-\Delta x)$ / $\Delta W(x+\Delta x)$	backward[b] $\Delta W(x-\Delta x)$ / $\Delta W(x+\Delta x)$	average $\Delta W(x-\Delta x)$ / $\Delta W(x+\Delta x)$	x (Å)	forward $\Delta W(x-\Delta x)$ / $\Delta W(x+\Delta x)$	backward[b] $\Delta W(x-\Delta x)$ / $\Delta W(x+\Delta x)$	average $\Delta W(x-\Delta x)$ / $\Delta W(x+\Delta x)$
−1.05	−0.344	−0.109	−0.238	0.60	0.105	0.105	0.105
	0.584	0.376	0.471		−0.142	−0.457	−0.320
−0.90	−0.182	−0.410	−0.307	0.75	0.135	0.649	0.338
	0.361	0.346	0.353		−0.102	−0.413	−0.278
−0.75	−0.413	−0.102	−0.278	0.90	0.346	0.361	0.353
	0.649	0.135	0.338		−0.410	−0.182	−0.307
−0.60	−0.457	−0.142	−0.320	1.05	0.376	0.584	0.471
	0.105	0.105	0.105		−0.109	−0.344	−0.238
−0.45	0.116	0.028	0.071	1.20	0.767		
	−0.015	0.084	0.033		−0.313		
−0.30	0.295	0.355	0.324	1.35	0.635		
	−0.203	−0.029	−0.122		−0.393		
−0.15	0.829	−0.391	0.571	1.50	0.492		
	−0.553	−0.037	−0.350		−0.406		
0.00	0.357	0.081	0.099	1.65	0.060		
	−0.081	−0.357	0.099		0.064		
0.15	−0.037	−0.553	−0.350	1.80	−0.392		
	0.391	0.829	0.571		0.557		
0.30	−0.029	−0.203	−0.122	1.95	−0.492		
	0.355	0.295	0.324		0.828		
0.45	0.084	−0.015	0.033				
	0.028	0.116	0.071				

[a] Δx equals 0.075 Å, i.e., half the distance between simulations. [b] The backward simulation results are obtained from the symmetry of the system; i.e., $W(x) = W(-x)$ and $\Delta W(x+\Delta x) = \Delta W(-x-\Delta x)$.

water as a solvent, the Born radius σ_w of Na^+ is about 2.25 Å, as indicated by ab initio calculations, by RISM-HNC integral equation calculations, and by MC simulations.[46] In the pore, the Born radius σ_p is about 2.15 Å, as estimated by ab initio

Table V

region III		region I		Region II	
x (Å)	$W(x)$	x (Å)	$W(x)$	x (Å)	$W(x)$
0.00	12.42	6.02	8.97	9.25	0.00
0.15	12.86	6.17	8.43	9.32	0.70
0.30	13.56	6.32	8.55	9.47	1.38
0.45	13.85	6.47	9.33	9.62	1.96
0.60	13.81	6.62	10.75	9.77	2.42
0.75	13.16	6.77	12.47	9.92	2.92
0.90	12.52	6.92	12.34	10.07	2.79
1.05	11.75	7.07	10.29	10.22	2.54
1.20	10.74	7.22	8.16	10.37	1.75
1.35	9.79	7.37	6.70	10.52	1.26
1.50	8.91	7.52	5.40	10.67	1.00
1.65	8.44	7.67	4.40	10.82	0.91
1.80	8.90	7.82	4.41	10.97	0.58
β-helix connector[a]		7.97	5.36	11.12	0.67
1.94	10.66	8.12	5.96	11.27	1.21
2.08	12.15	8.27	6.68	11.42	2.20
2.23	12.84	8.42	6.11	11.57	3.40
2.37	12.97	8.57	4.28	11.72	3.83
2.52	12.67	8.72	2.36	11.87	3.69
2.66	11.78	8.87	0.74	12.02	3.46
2.81	10.51	9.02	0.15	12.17	3.49
2.95	9.07	9.17	0.04	12.32	3.70
3.10	8.44			12.47	3.87
3.25	8.72			12.62	3.85
3.39	9.76			12.77	4.00
3.54	11.22			12.92	4.67
3.68	12.45			13.07	5.19
3.83	12.95			13.22	5.46
3.97	12.87			13.37	5.64
4.12	12.43			13.52	5.84
4.26	11.33			13.67	6.04
4.41	9.96			13.82	6.01
4.55	8.68			13.97	6.76
4.65	8.44			14.12	7.45
4.80	8.72			14.27	7.66
4.94	9.76			14.42	7.31
5.09	11.22			14.57	7.41
5.23	12.45				
5.38	12.95				
5.52	12.87				
5.67	12.43				
5.81	11.33				
5.91	10.51				

[a] The connection between region III and the β-helix simulation was adjusted so there are minima at x = 3.10 and 4.65 Å. The zero at 9.25 Å is an arbitrary origin for the free energy profile.

calculations on model peptides and molecular dynamics simulations.[46] Experimentally, it has been found that the solvation mechanism in the channel can be understood in terms of the solvation in dimethylformamide (DMF).[43] The experimental transfer free energy from water to DMF for the Na^+ ion is −2.5 kcal/mol.[47] Using solvent-dependent Born radii, the electrostatic free energy of transfer is

$$\Delta\mu_{DMF} - \Delta\mu_w = \frac{Q^2}{2\sigma_{DMF}}\left(\frac{1}{\epsilon_{DMF}} - 1\right) - \frac{Q^2}{2\sigma_w}\left(\frac{1}{\epsilon_{DMF}} - 1\right) \quad (A.2)$$

The dielectric constant for bulk water is 78.4 and for liquid DMF is 37.2.[48] This yields a negative free energy of transfer of −2.4 kcal/mol. While the agreement is partly fortuitous, this example illustrates the fact that it is possible to have a favorable transfer of an ion to a lower dielectric medium as long as the short-range microscopic interactions give rise to a smaller "Born radius". Thus, the transfer free energy is a balance between "localized properties", σ_w and σ_{DMF}, and "delocalized properties", ϵ_w and ϵ_{DMF}.

(46) Roux, B. Theroetical Studies of Ion Transport in the Gramicidin Channel. Ph.D. Thesis, Harvard University, 1990.
(47) Cox, B. G.; HeΔWig, G. R.; Parker, A. J.; Watts, D. W. *Aust. J. Chem.* **1974**, *27*, 477.
(48) Bass, S. J.; Nathan, W. I.; Meighan, R. M.; Cole, R. H. *J. Phys. Chem.* **1964**, *68*, 509.

The absolute free energy estimated by eq A.1 is extremely sensitive to the values of the radius of the ion in the bulk and in the pore. The exact value to be used has an empirical character and depends on the local solvent structure around the ion. From the above analysis it is clear that σ_w is not equal to σ_p and that, unless an accurate procedure is available to determine the solvent-dependent radii, the Born model is not useful to predict the transfer free energy between different environments. Assumptions about the Born radius in bulk water and in the channel may have led to an overestimated electrostatic "images charge" energy barrier.[35,36]

To estimate the effect of the finite size of the cylindrical simulation system on the free energy profile along the channel axis, the particular choice of a Born radius for the ion has no effect on the final result and the use of continuum electrostatics is valid. The free energy of transfer from bulk water to the center of an infinitely long aqueous cylinder of radius R is given by[34]

$$\Delta\mu_w^{cylinder} - \Delta\mu_w^{bulk} = \frac{1}{\pi}\int_0^\infty dx \frac{\alpha x K_0(x) K_1(x)}{1 - \alpha x I_0(x) K_1(x)} \quad (A.3)$$

where I_0, K_0, and K_1 are modified Bessel functions of the first and second kind and α is defined as $(1 - 1/\epsilon_w)$. For a cylinder radius R of 10.5 Å, this expression yields a free energy loss of about 4.24 kcal/mol. The Born radius of the ion in water, σ_w, does not appear in the finite size correction.

To estimate the free energy loss in the finite model membrane, the length of the pore is assumed to be much longer than its radius. The pore system is modeled as a series of concentric cylinders with various dielectric constants to represent successively the pore (ϵ_1), the channel (ϵ_2), and the membrane (ϵ_3):

$$\epsilon_1 \quad 0 \le r \le R_1 \qquad \epsilon_2 \quad R_1 \le r \le R_2 \qquad \epsilon_3 \quad R_2 \le r \le \infty \quad (A.4)$$

In the infinite system, the dielectric constant of the membrane ϵ_3 is equal to 2 to represent the hydrocarbon membrane. In the finite system, it is equal to 1 to represent vacuum. The outer radius R_2 is 10.5 Å in the system. The free energy loss is calculated as the difference of electrostatic solvation energy between the two systems; i.e.,

$$\Delta\Delta\mu_p = \Delta\mu_p(\epsilon_3 = 1) - \Delta\mu_p(\epsilon_3 = 2) \quad (A.5)$$

The solution to the electrostatic problem is given in detail by[35]

$$\Delta\Delta\mu_p = \frac{Q_2}{\epsilon_1 \pi R_1}\int_0^\infty dx\, [B_1(x;\epsilon_3 = 1) - B_1(x;\epsilon_3 = 2)] \quad (A.6)$$

where the function B_1 is defined by

$$B_1(x;\epsilon_3) = \kappa_1(x)\left[1 + \frac{\lambda_1 \phi_1^2(x) \kappa_2(xR_2/R_1)}{\kappa_1(x) - \kappa_2(xR_2/R_1)(1 - \phi_1(x))(1 - \lambda_1\phi_1(x))}\right] \quad (A.7)$$

where

$$\lambda_1 = \epsilon_2/\epsilon_1 \quad \text{and} \quad \lambda_2 = \epsilon_3/\epsilon_2 \quad (A.8)$$

$$\phi_\alpha(x) = [1 - (1 - \lambda_a) x R_\alpha I_0(x)]^{-1} \quad (A.9)$$

$$\kappa_\alpha(x) = (1 - \lambda_\alpha) x R_\alpha K_0(x) K_1(x) \phi_\alpha(x) \quad (A.10)$$

The Born radius of the ion in the pore σ_p does not appear in the problem.

Numerical calculations show that, using the values $\epsilon_1 = 40$, $\epsilon_2 = 5$, $R_1 = 4.0$ Å, and $R_2 = 10.5$ Å, the free energy loss due to the absence of any explicit membrane is 3.0–4.0 kcal/mol. Further testing showed that this estimate does not depend strongly on the values chosen for the parameters. The radius of the pore R_1 was

varied from 3 to 5 Å with no significant effects (less than ±0.5 kcal/mol). A variation of the dielectric constant of the pore ϵ_1 from 1 to 80 had little effect (about ±0.7 kcal/mol), although the value of 40, corresponding to liquid DMF, is probably an appropriate estimate. The most sensitive parameter is the dielectric constant of the channel "wall", located between R_1 and R_2. It is mostly constituted of nonpolar side chains, and the dielectric constant should be 3–5 from recent estimates.[49] Use of a value of 25 for ϵ_2 decreased the free energy loss by 1.5 kcal/mol.

The free energy loss in the finite pore is remarkably close to the loss of free energy in the finite aqueous cylinder, though the origin of the free energy loss is different in the two cases. In the aqueous cylinder, the dielectric shielding is high and the free energy is "concentrated" close to the ion. In the membrane, a pore of radius 3–5 Å with a dielectric constant of 80 cannot provide sufficient dielectric shielding and the electrostatic energy density arising from the hydrocarbon region is comparable to the free energy loss in a finite aqueous cylinder. These considerations based on continuum electrostatics show that the free energy losses due to the finiteness of the system in the aqueous region and in the membrane region nearly cancel each other in the present calculations. Thus, no electrostatic correction was added to the free energy profile calculated from the finite cylindrical system with the free energy perturbation method.

(49) Gilson, M. K.; Honig, B. *Proteins: Struct., Funct., Genet.* **1988**, *4*, 7.

(50) Partenskii, M. B.; Jordan, P. C. *J. Phys. Chem.* **1992**, *96*, 3906.

Appendix B. Simulation Results

In Tables II–IV we give all the free energy perturbation elements obtained from the simulations with the full gramicidin A channel system in the three regions of interest. The values $W(x+\Delta x)$ and $W(x-\Delta x)$ were calculated from simulations with the ion constrained at position x, as described in the text. The simulation procedure used to produce the successive increasing and decreasing values of x generated the forward and backward sets of perturbation elements.

Appendix C. Complete Free Energy Profile for the Na^+ Ion in the Gramicidin A Channel

In Table V we give the complete free energy profile of the Na^+ ion in the right-handed dimer obtained by assembling the three regions considered in the present study and a connector constructed from the periodic β-helix, as described in the text. For example,

$$W(6.32) = W(6.17) + \Delta W(6.17 \rightarrow 6.17+\Delta x) - \Delta W(6.32 \rightarrow 6.32-\Delta x)$$

$$W(6.32) = 8.43 + 0.011 - (-0.106)$$

$$W(6.32) = 8.546$$

where the numbers are taken from Table II.